JACS
JOURNAL OF THE AMERICAN CHEMICAL SOCIETY
Communication
pubs.acs.org/JACS

Hierarchical Self-Assembly: Well-Defined Supramolecular Nanostructures and Metallohydrogels via Amphiphilic Discrete Organoplatinum(II) Metallacycles

Xuzhou Yan,[†,‡] Shijun Li,[‡,§] Timothy R. Cook,[‡] Xiaofan Ji,[†] Yong Yao,[†] J. Bryant Pollock,[‡] Yanhui Shi,[∥,‡] Guocan Yu,[†] Jinying Li,[†] Feihe Huang,*[,†] and Peter J. Stang*[,‡]

[†]Center for Chemistry of High-Performance and Novel Materials, Department of Chemistry, Zhejiang University, Hangzhou, Zhejiang 310027, P. R. China

[‡]Department of Chemistry, University of Utah, 315 South 1400 East, Room 2020, Salt Lake City, Utah 84112, United States

[§]College of Material, Chemistry and Chemical Engineering, Hangzhou Normal University, Hangzhou, Zhejiang 310036, P. R. China

[∥]School of Chemistry and Chemical Engineering, Jiangsu Normal University, Xuzhou, Jiangsu 221116, P. R. China

Supporting Information

ABSTRACT: Metallacyclic cores provide a scaffold upon which pendant functionalities can be organized to direct the formation of dimensionally controllable nanostructures. Because of the modularity of coordination-driven self-assembly, the properties of a given supramolecular core can be readily tuned, which has a significant effect on the resulting nanostructured material. Herein we report the efficient preparation of two amphiphilic rhomboids that can subsequently order into 0D micelles, 1D nanofibers, or 2D nanoribbons. This structural diversity is enforced by three parameters: the nature of the hydrophilic moieties decorating the parent rhomboids, the concentration of precursors during self-assembly, and the reaction duration. These nanoscopic constructs further interact to generate metallohydrogels at high concentrations, driven by intermolecular hydrophobic and $\pi-\pi$ interactions, demonstrating the utility of coordination-driven self-assembly as a first-order structural element for the hierarchical design of functional soft materials.

The motivation for artificial hierarchical design originates from elegant examples in biology such as polypeptides, whose covalently tethered amino acid chains fold as a result of hydrogen bonding to afford secondary order (α-helices, β-sheets, etc.) and further self-organize into higher-order supramolecular architectures as a result of hydrophobic/hydrophilic effects (so-called tertiary structure), ultimately delivering complex macromolecules capable of highly specific functionalities.[1] Inspired by such natural processes, chemists have exploited weak molecular interactions as the impetus for the self-assembly of nanoscale materials with unprecedented structures and intriguing functions,[2] thereby defining the fundamental science behind supramolecular engineering.[3] The interactions among amphiphilic molecules featuring hydrophilic and hydrophobic segments particularly lend themselves to the rational design of diverse aggregation-based supramolecular nanostructures such as micelles, vesicles, ribbons, nanotubes, etc., that are structurally complex but synthetically facile via self-assembly.[4] In the past decade, significant research on the self-assembly of surfactants, phospholipids, amphiphilic block polymers, rigid−flexible block molecules, and macrocyclic amphiphiles has established a host of dimension-controlled nanostructures for various applications.[4d,5] Zhang and co-workers recently developed the concept of supra-amphiphiles, wherein parent amphiphiles are functionalized by either non-covalent interactions or dynamic covalent bonds.[6] In this way, multiple interactions can work in concert to afford increasingly complex structures.

The spontaneous formation of metal−ligand bonds is the basis of a well-established methodology for the construction of supramolecular coordination complexes (SCCs) using a process called coordination-driven self-assembly.[7] From the wide range of metals and ligands that are compatible with this technique, a sizable library of discrete 2D and 3D SCCs has emerged over the years, spanning multiple synthetic methodologies that are unified under the approach of *directional bonding*.[8] Exemplary structures comprising phosphine-capped Pt(II) nodes with rigid organic donors have been used to illustrate how the directionalities of the precursors dictate specific structural outcomes.[8a,9] The maturation of this field has witnessed adaptations of SCCs for host−guest chemistry,[10] catalysis,[11] molecular conductance,[12] molecular flasks,[13] bioengineering,[14] and so on.

Since the formation of metal−ligand bonds can occur in parallel with other intermolecular interactions, it is possible to design systems that mimic the hierarchical ordering found in natural systems, as mentioned above. That said, metallacyclic amphiphiles based on discrete SCC cores are underexplored yet represent a potentially powerful means to expand supramolecular engineering. Herein we report the design and synthesis of functionalized dicarboxylate ligands amenable to coordination-driven self-assembly and the subsequent formation of amphiphilic organoplatinum(II) metallacycles, which form diverse, well-defined nanostructures (0D micelles, 1D nanofibers, and 2D nanoribbons) and metallohydrogels depending on the conditions involved in their self-assembly processes.

Received: July 5, 2013
Published: August 8, 2013

dx.doi.org/10.1021/ja406877b | J. Am. Chem. Soc. 2013, 135, 14036−14039

The Stang group has previously explored carboxylate-based ligands that assemble with Pt(II) acceptors to afford neutral, planar organoplatinum(II) metallacycles containing hydrophobic cores.[15] These designs have inspired the current work, in which the hydrophobic cores are decorated with poly(ethylene glycol) (PEG) units to furnish two amphiphilic discrete metallacycles, **1** and **2** (Scheme 1), that share the same rhombic

Scheme 1. Self-Assembly of (a) 3−5 To Give Amphiphilic Rhomboids 1 and 2 and (b) 1 and 2 To Give 0D Micelles, 1D Nanofibers, and 2D Nanoribbons

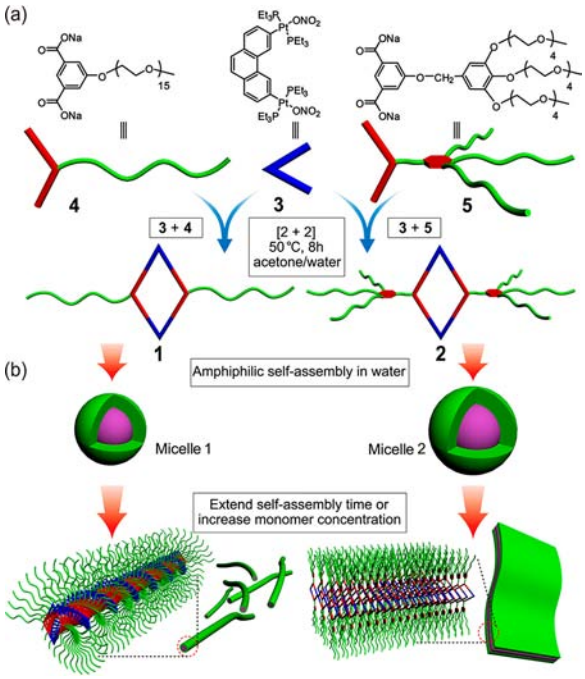

core and have similar molecular weights (3787.85 Da for **1** and 3855.89 Da for **2**) but different structural hydrophilic segments, namely, a linear PEG chain in **1** and branched PEG group in **2** (Scheme 1a). When a 1:1 mixture of 120° ligand **4** or **5** and the 60° organoplatinum(II) acceptor 3,6-bis[*trans*-Pt-$(PEt_3)_2(NO_3)_2$]phenanthrene (**3**) was first dissolved in D_2O/acetone-d_6 and then isolated and redissolved in acetone-d_6 at 50 °C for 8 h, [2 + 2] self-assembly furnished amphiphilic rhomboids with hydrophilic segments at the obtuse vertices (Scheme 1a). ^{1}H and ^{31}P NMR analyses of the reaction mixtures supported the formation of discrete, highly symmetric species (Figure 1 and Figure S17 in the Supporting Information). The ^{31}P{^{1}H} NMR spectrum of **1**, for example, possesses a lone sharp singlet at ∼14.10 ppm with concomitant ^{195}Pt satellites (J_{Pt-P} = 2909.9 Hz), consistent with a single phosphorus environment (Figure 1b). This peak is shifted upfield relative to that of acceptor **3** by ∼2.20 ppm. The spectrum of **2** similarly possesses a single sharp peak with Pt satellites (Figure 1c).

Electrospray ionization time-of-flight mass spectrometry (ESI-TOF-MS) provided evidence for the stoichiometry of formation of rhomboids **1** and **2**. In the mass spectrum of **1**, nine peaks were found that were consistent with the assignment of a [2 + 2] assembly (Figure S14). Among these were a peak at *m*/*z* 969.89 corresponding to $[M + 4Na]^{4+}$ (Figure 2a). For rhomboid **2**, six such peaks were found (Figure S17), such as the peak at *m*/*z* 1928.77 corresponding to $[M + 2H]^{2+}$ (Figure 2b). All of the

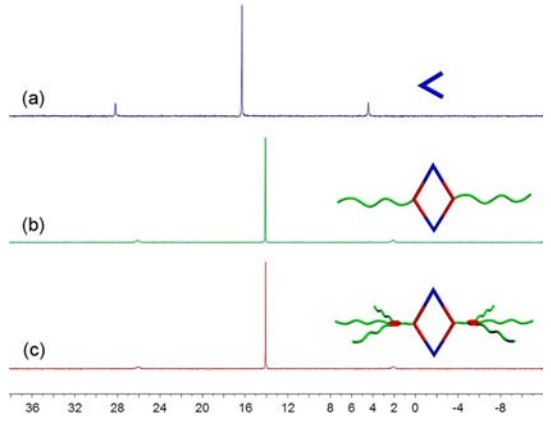

Figure 1. ^{31}P{^{1}H} NMR spectra (acetone-d_6, room temperature, 121.4 MHz) of (a) 60° acceptor **3**, (b) rhomboid **1**, and (c) rhomboid **2**.

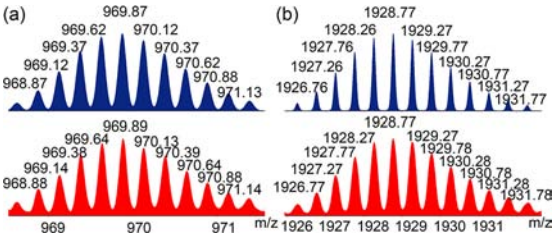

Figure 2. Experimental (red) and calculated (blue) ESI-TOF-MS spectra of (a) **1** $[M + 4Na]^{4+}$ and (b) **2** $[M + 2H]^{2+}$.

peaks were isotopically resolved and agreed very well with their calculated theoretical distributions (Figure 2).

Aqueous solutions of rhomboids **1** and **2** showed clear evidence of the Tyndall effect (Figure 3 insets), indicating the

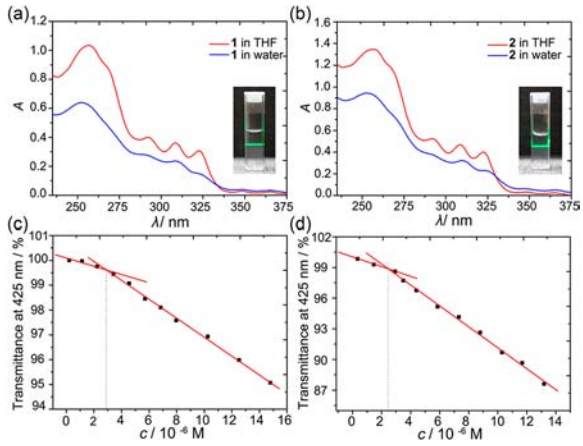

Figure 3. (a, b) UV−vis absorption spectra of (a) **1** and (b) **2** in THF (red) and water (blue). Insets: Tyndall effect of (left) **1** and (right) **2**. [**1**] = [**2**] = 1.00 × 10^{-5} M. (c, d) Concentration-dependent optical transmittance of (c) **1** and (d) **2** in water.

existence of nanoaggregates. This scattering phenomenon did not occur for solutions of the free ligands, which lack the hydrophobic cores required for formation of amphiphilic constructs (Figure S24). This aggregation behavior was further studied using UV−vis spectroscopy. The intensities of the broad absorption manifolds of **1** and **2** significantly decreased when 1.00 × 10^{-5} M solutions were prepared in water versus tetrahydrofuran (THF). This decrease is consistent with the

dx.doi.org/10.1021/ja406877b | J. Am. Chem. Soc. 2013, 135, 14036−14039

formation of aggregates, reducing the number of absorbing species in solution.[16] Furthermore, plots of optical transmittance versus concentration at 425 nm revealed two regimes, indicating critical aggregation concentrations (CACs) of 2.82×10^{-6} M for **1** and 2.49×10^{-6} M for **2** (Figures 3 and S18).

Transmission electron microscopy (TEM) was used to visualize the aggregates of amphiphilic rhomboids **1** and **2**. Dark-gray spherical micellar structures formed by **1** were observed at concentrations exceeding the CAC (Figure 4a).

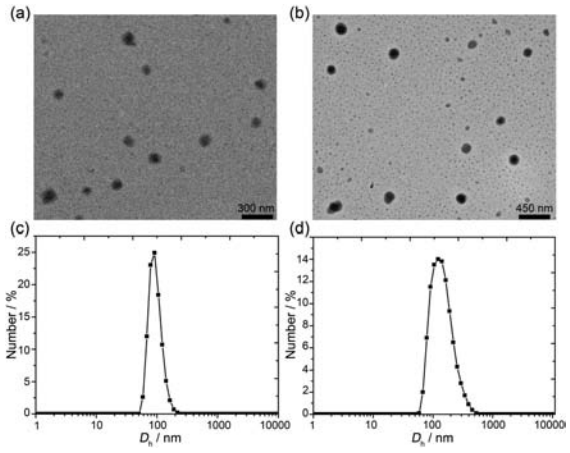

Figure 4. (a, b) TEM images and (c, d) DLS data at a scattering angle of 90° for the self-assembled micellar structures formed by (c) **1** and (d) **2** in water. $[\mathbf{1}]_0 = [\mathbf{2}]_0 = 5.00 \times 10^{-6}$ M.

The diameters of these micelles ranged from 50 to 100 nm with an average of ~90 nm (Figures 4a and S19a). Dynamic light scattering (DLS) experiments performed with a 5.00×10^{-6} M aqueous solution of **1** over a scattering angle of 90° agreed with these metrics, showing a narrow size distribution (Figure 4c). The average hydrodynamic diameter (D_h) of **1** was observed to be 92 nm, in accordance with the TEM results. Rhomboid **2** also formed micellar aggregates with diameters of 70−150 nm at a concentration of 5.00×10^{-6} M (Figures 4b and S19b). Similar DLS experiments showed an average micellar diameter of ~120 nm (Figure 4d), consistent with the dimensions found by TEM.

Since **1** and **2** contain robust, well-defined cores, the possibility of higher-order structures resulting from additional intermolecular interactions was explored. When the concentration of the amphiphiles was increased from 5.00×10^{-6} to 5.00×10^{-5} M in water, TEM images revealed that the morphology of the resulting aggregates underwent marked changes. Amphiphilic rhomboid **1** self-assembled into fibrous nanostructures (Figure 5a). The lack of shape contrast between the peripheral and central parts of the fibers attests to their solid, uniform disposition (Figure 5b). The nanofibers had widths of 10−50 nm and lengths of ~1 μm, suggesting a 1D propagation process. The formation of 1D fibers is consistent with bolaamphiphile-type packing, wherein the hydrophobic cores are further ordered by offset $\pi-\pi$ stacking of the planar rhombic frameworks and the PEG groups extend radially from the cylindrical framework (Scheme 1b). The minimum diameter of the thin nanofibers was ~10 nm. Molecular modeling of **1** revealed a maximum PEG tip-to-tip distance of ~12.8 nm, in good agreement with the observed diameters of single fibers (Figure S23a). From these dimensions, it appears that micelle **1** further aggregates to form cylindrical fibers that subsequently form laterally associated fiber bundles of one to five strands. Further experiments revealed that these

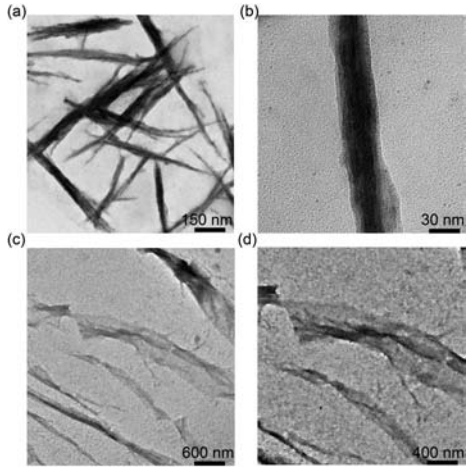

Figure 5. (a, c) Low- and (b, d) high-magnification TEM images of self-assembled nanostructures formed in water: (a, b) nanofibers of **1**; (c, d) nanoribbons of **2**. $[\mathbf{1}]_0 = [\mathbf{2}]_0 = 5.00 \times 10^{-5}$ M.

bundles are a thermodynamic sink, as the micelles of **1** formed in 5.00×10^{-6} M solutions were converted to nanofibers upon standing over the course of 1 week (Figure S20b).

Analogous studies of rhomboid **2** at a concentrations of 5.00×10^{-5} M in water similarly suggested that the spherical micelles are a kinetic product. In the case of **2**, TEM experiments revealed that the rhomboids ultimately formed 2D nanoribbons (Figures 5c and S21a). To gain further insight into the nature of these 2D nanostructures, additional UV−vis spectroscopy experiments were run. In THF, solutions of **2** showed absorption features consistent with monomeric rhomboids. Solutions of **2** in water revealed 4 nm red shifts of the bands at 292, 309, and 323 nm with concomitant attenuation of the intensity relative to that in THF (Figure 2b). This is a characteristic of J-type aggregates and further supports the higher-order assembly of rhomboids into nanoribbons (Scheme 1b).[6b] As with **1**, the spherical micelles of **2** produced initially at lower concentrations eventually formed to 2D nanoribbons (Figure S21b).

In addition to the interesting self-assembly behaviors of the amphiphilic rhomboids **1** and **2** in water, it is worth noting that both can form metallohydrogels (Figure 6a,c). The critical gel concentrations (the lowest amounts of rhomboid needed to sustain gel formation) were determined to be 4.56 wt % for **1** and

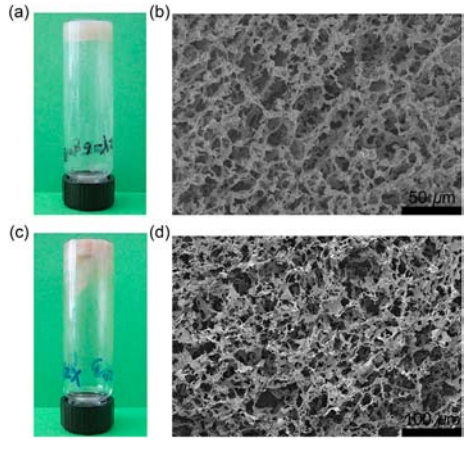

Figure 6. (a, c) Photographs and (b, d) SEM images of the metallohydrogels formed by (a, b) **1** and (c, d) **2**.

dx.doi.org/10.1021/ja406877b | J. Am. Chem. Soc. 2013, 135, 14036−14039

5.55 wt % for **2**. The morphologies of the xerogels **1** and **2**, which were prepared by freeze-drying methodology, were examined by scanning electron microscopy (SEM), which revealed similar interconnected porous structures (Figure 6b,d), in which the fibrous 1D and 2D materials intertwined to furnish 3D networks responsible for the observed gelations (Figure 6a,c). These formations stem from the dual hydrophobic and $\pi-\pi$ interactions that both rhomboids can exhibit. Since the use of metallo-based gelators incorporates organoplatinum(II) nodes throughout the gel, this design establishes routes to functional soft materials exploiting the unique properties of Pt(II) centers.[17]

In summary, by means of a *directional-bonding approach*, the two amphiphilic rhomboids **1** and **2** were prepared with high efficiency. Furthermore, well-defined nanostructures such as 0D micelles, 1D nanofibers, and 2D nanoribbons were obtained by selecting the conditions of self-assembly. Such nanostructural diversity was achieved by elaborately tuning the hydrophilic segments of the rhombic building blocks while maintaining control over the solvent, reaction time, and concentration, all of which can be adjusted easily. Notably, **1** and **2** formed metallohydrogels at high concentration driven by hydrophobic and $\pi-\pi$ interactions. This design exploits hierarchical assembly with multiple interactions working in concert to deliver complex materials. The first level of organization is the spontaneous formation of metal−ligand bonds to generate discrete cores. The amphiphilic nature of these SCCs motivates secondary ordering into micelles, which can further assemble by a third intermolecular interaction wherein the extended π systems of the SCC cores can interact to give 1D or 2D ordering into fibers or ribbons. This three-level self-assembly allows both materials to form porous 3D networks capable of supporting metallohydrogel formation. The unification of coordination-driven self-assembly, amphiphilic self-assembly, and hydrogel formation defines a new approach to the engineering of soft materials with fine control over the dimensionality of the resultant nanostructures. Given the potential applications in biological systems and materials science, we expect this technique to unlock interesting new designs incorporating metal centers into complex multidimensional materials.

■ ASSOCIATED CONTENT

Supporting Information

Experimental details and additional data. This material is available free of charge via the Internet at http://pubs.acs.org.

■ AUTHOR INFORMATION

Corresponding Author

fhuang@zju.edu.cn; stang@chem.utah.edu

Notes

The authors declare no competing financial interest.

■ ACKNOWLEDGMENTS

F.H. thanks the National Basic Research Program of China (2013CB834502), the National Natural Science Foundation of China (91027006, 21125417), and the Fundamental Research Funds for the Central Universities (2012QNA3013) for support. P.J.S. thanks the NSF (1212799) for support.

■ REFERENCES

(1) Bryson, J. W.; Betz, S. F.; Lu, H. S.; Suich, D. J.; Zhou, H. X.; O'Neil, K. T.; DeGrado, W. F. *Science* **1995**, *270*, 935.

(2) (a) Hartgerink, J. D.; Beniash, E.; Stupp, S. I. *Science* **2001**, *294*, 1684. (b) Wang, Y.; Xu, H.; Zhang, X. *Adv. Mater.* **2009**, *21*, 2849. (c) Yan, X.; Wang, F.; Zheng, B.; Huang, F. *Chem. Soc. Rev.* **2012**, *41*, 6042. (d) Banerjee, S.; König, B. *J. Am. Chem. Soc.* **2013**, *135*, 2967.

(3) (a) Meng, F.; Zhong, Z.; Feijen, J. *Biomacromolecules* **2009**, *10*, 197. (b) Hosono, N.; Kajitani, T.; Fukushima, T.; Ito, K.; Sasaki, S.; Takata, M.; Aida, T. *Science* **2010**, *330*, 808. (c) Kim, P.; Abkarian, M.; Stone, H. A. *Nat. Mater.* **2011**, *10*, 952. (d) Fenske, T.; Korth, H.-G.; Mohr, A.; Schmuck, C. *Chem.—Eur. J.* **2012**, *18*, 738. (e) Yan, X.; Xu, D.; Chi, X.; Chen, J.; Dong, S.; Ding, X.; Yu, Y.; Huang, F. *Adv. Mater.* **2012**, *24*, 362.

(4) (a) Moffitt, M.; Khougaz, K.; Eisenberg, A. *Acc. Chem. Res.* **1996**, *29*, 95. (b) Jiang, Y.; Wang, Y.; Ma, N.; Wang, Z.; Smet, M.; Zhang, X. *Langmuir* **2007**, *23*, 4029. (c) Zhou, Y.; Yan, D. *Chem. Commun.* **2009**, 1172. (d) Hu, J.; Wu, T.; Zhang, G.; Liu, S. *J. Am. Chem. Soc.* **2012**, *134*, 7624.

(5) (a) Mai, Y.; Eisenberg, A. *J. Am. Chem. Soc.* **2010**, *132*, 10078. (b) Kim, H.-J.; Kim, T.; Lee, M. *Acc. Chem. Res.* **2011**, *44*, 72. (c) Guo, D.-S.; Wang, K.; Wang, Y.-X.; Liu, Y. *J. Am. Chem. Soc.* **2012**, *134*, 10244. (d) Yu, G.; Xue, M.; Zhang, Z.; Li, J.; Han, C.; Huang, F. *J. Am. Chem. Soc.* **2012**, *134*, 13248. (e) Yao, Y.; Xue, M.; Chen, J.; Zhang, M.; Huang, F. *J. Am. Chem. Soc.* **2012**, *134*, 15712. (f) Xu, F.; Wang, H.; Zhao, J.; Liu, X.; Li, D.; Chen, C.; Ji, J. *Macromolecules* **2013**, *46*, 4235. (g) Liu, Y.; Yu, C.; Jin, H.; Jiang, B.; Zhu, X.; Zhou, Y.; Lu, Z.; Yan, D. *J. Am. Chem. Soc.* **2013**, *135*, 4765. (h) Fenske, M. T.; Meyer-Zaika, W.; Korth, H.-G.; Vieker, H.; Turchanin, A.; Schmuck, C. *J. Am. Chem. Soc.* **2013**, *135*, 8342.

(6) (a) Wang, C.; Wang, Z.; Zhang, X. *Acc. Chem. Res.* **2012**, *45*, 608. (b) Liu, K.; Yao, Y.; Wang, C.; Liu, Y.; Li, Z.; Zhang, X. *Chem.—Eur. J.* **2012**, *18*, 8622.

(7) (a) Fujita, M.; Tominaga, M.; Hori, A.; Therrien, B. *Acc. Chem. Res.* **2005**, *38*, 369. (b) Oliveri, C. G.; Ulmann, P. A.; Wiester, M. J.; Mirkin, C. A. *Acc. Chem. Res.* **2008**, *41*, 1618. (c) Northrop, B. H.; Zheng, Y.-R.; Chi, K.-W.; Stang, P. J. *Acc. Chem. Res.* **2009**, *42*, 1554. (d) De, S.; Mahata, K.; Schmittel, M. *Chem. Soc. Rev.* **2010**, *39*, 1555. (e) Adarsh, N. N.; Dastidar, P. *Chem. Soc. Rev.* **2012**, *41*, 3039. (f) Kreno, L. E.; Leong, K.; Farha, O. K.; Allendorf, M.; Van Duyne, R. P.; Hupp, J. T. *Chem. Rev.* **2012**, *112*, 1105. (g) Cook, T. R.; Zheng, Y.-R.; Stang, P. J. *Chem. Rev.* **2013**, *113*, 734.

(8) (a) Chakrabarty, R.; Mukherjee, P. S.; Stang, P. J. *Chem. Rev.* **2011**, *111*, 6810. (b) Sun, Q.-F.; Sato, S.; Fujita, M. *Nat. Chem.* **2012**, *4*, 330. (c) Smulders, M. M.; Riddell, I. A.; Browne, C.; Nitschke, J. R. *Chem. Soc. Rev.* **2013**, *42*, 1728.

(9) (a) Yang, H.-B.; Ghosh, K.; Zhao, Y.; Northrop, B. H.; Lyndon, M. M.; Muddiman, D. C.; White, H. S.; Stang, P. J. *J. Am. Chem. Soc.* **2008**, *130*, 389. (b) Lee, J.; Ghosh, K.; Stang, P. J. *J. Am. Chem. Soc.* **2009**, *131*, 12028. (c) Zheng, Y.-R.; Lan, W.-J.; Wang, M.; Cook, T. R.; Stang, P. J. *J. Am. Chem. Soc.* **2011**, *133*, 17045.

(10) (a) Yang, H.-B.; Ghosh, K.; Northrop, B. H.; Zheng, Y.-R.; Lyndon, M. M.; Muddiman, D. C.; Stang, P. J. *J. Am. Chem. Soc.* **2007**, *129*, 14187. (b) Li, S.; Huang, J.; Cook, T. R.; Pollock, J. B.; Kim, H.; Chi, K.-W.; Stang, P. J. *J. Am. Chem. Soc.* **2013**, *135*, 2084.

(11) (a) Pluth, M. D.; Bergman, R. G.; Raymond, K. N. *Acc. Chem. Res.* **2009**, *42*, 1650. (b) Brown, C. J.; Miller, G. M.; Johnson, M. W.; Bergman, R. G.; Raymond, K. N. *J. Am. Chem. Soc.* **2011**, *133*, 11964.

(12) Kiguchi, M.; Inatomi, J.; Takahashi, Y.; Tanaka, R.; Osuga, T.; Murase, T.; Fujita, M.; Tada, T.; Watanabe, S. *Angew. Chem., Int. Ed.* **2013**, *52*, 6202.

(13) Inokuma, Y.; Kawano, M.; Fujita, M. *Nat. Chem* **2011**, *3*, 349.

(14) Jung, H.; Dubey, A.; Koo, H. J.; Vajpayee, V.; Cook, T. R.; Kim, H.; Kang, S. C.; Stang, P. J.; Chi, K.-W. *Chem.—Eur. J.* **2013**, *19*, 6709.

(15) Mukherjee, P. S.; Das, N.; Kryschenko, Y. K.; Arif, A. M.; Stang, P. J. *J. Am. Chem. Soc.* **2004**, *126*, 2464.

(16) (a) Schenning, A. P. H. J.; Jonkheijm, P.; Peeters, E.; Meijer, E. W. *J. Am. Chem. Soc.* **2001**, *123*, 409. (b) Lee, E.; Kim, J.-K.; Lee, M. *Angew. Chem., Int. Ed.* **2009**, *48*, 3657.

(17) (a) Xu, X.-D.; Zhang, J.; Chen, L.-J.; Zhao, X.-L.; Wang, D.-X.; Yang, H.-B. *Chem.—Eur. J.* **2012**, *18*, 1659. (b) Xu, X.-D.; Zhang, J.; Yu, X.; Chen, L.-J.; Wang, D.-X.; Yi, T.; Li, F.; Yang, H.-B. *Chem.—Eur. J.* **2012**, *18*, 16000.